

*Cardiovascular, Pulmonary and Renal Pathology*

# Interferon- $\gamma$ Induces Chronic Active Myocarditis and Cardiomyopathy in Transgenic Mice

Kurt Reifenberg,\* Hans-Anton Lehr,<sup>†</sup>  
Michael Torzewski,<sup>‡</sup> Gisela Steige,\* Elena Wiese,\*  
Ines Küpper,\* Christoph Becker,<sup>§</sup> Sibylle Ott,<sup>¶</sup>  
Petra Nusser,<sup>¶</sup> Ken-Ichi Yamamura,<sup>||</sup>  
Gerd Rechtsteiner,\*\* Tobias Warger,\*\*  
Andrea Pautz,<sup>††</sup> Hartmut Kleinert,<sup>††</sup>  
Albrecht Schmidt,<sup>‡‡</sup> Burkert Pieske,<sup>‡‡</sup>  
Philip Wenzel,<sup>§§</sup> Thomas Münzel,<sup>§§</sup>  
and Jürgen Löhler<sup>¶¶</sup>

From the Central Laboratory Animal Facility,\* the Institute of Clinical Chemistry and Laboratory Medicine,<sup>‡</sup> the First Medical Clinic,<sup>§</sup> the Institute of Immunology,\*\* the Institute of Pharmacology,<sup>¶¶</sup> and the Second Medical Clinic,<sup>§§</sup> Johannes Gutenberg-University, Mainz, Germany; the Department of Cardiology and Pneumology,<sup>‡‡</sup> University of Goettingen, Goettingen, Germany; Laboratory Animal Research Unit,<sup>¶¶</sup> University of Ulm, Ulm, Germany; Heinrich Pette Institute for Experimental Virology and Immunology,<sup>¶¶</sup> Hamburg, Germany; Institut Universitaire de Pathologie,<sup>†</sup> Centre Hospitalier Universitaire Vaudois, Lausanne, Switzerland; and the Institute of Molecular Embryology and Genetics,<sup>||</sup> Kumamoto, Japan

**Chronic heart failure is associated with an activation of the immune system characterized among other factors by the cardiac synthesis and serum expression of proinflammatory cytokines. There is unequivocal clinical and experimental evidence that the cytokine tumor necrosis factor- $\alpha$  is involved in the development of chronic heart failure, but a putative cardiotoxic potential of the proinflammatory cytokine interferon (IFN)- $\gamma$  remains primarily unknown. To investigate this issue we analyzed the cardiac phenotype of SAP-IFN- $\gamma$  transgenic mice, which constitutively express IFN- $\gamma$  in their livers and hence exhibit high circulating serum levels of this cytokine. SAP-IFN- $\gamma$  mice spontaneously developed chronic active myocarditis, characterized by the infiltration of not only CD4<sup>+</sup> and CD8<sup>+</sup> T cells but also Mac2<sup>+</sup> (galectin 3<sup>+</sup>) macrophages and CD11c<sup>+</sup> dendritic cells, eventually culminating in cardiomyopathy. Echocardiographic analyses exhibited a left ventricular dilation and impaired systolic function induced by IFN- $\gamma$  over-**

**expression. IFN- $\gamma$ -mediated cardiotoxicity was associated with high-level cardiac transcription of the proinflammatory cytokines tumor necrosis factor- $\alpha$  and interleukin-12 and the macrophage-attracting chemokines MCP1 and MIP1- $\alpha$ . Myotoxic IFN- $\gamma$  effects could not be detected in smooth or striated muscle tissue, suggesting cardiomyocellular specificity of the toxic IFN- $\gamma$  effect. The precise mechanism of IFN- $\gamma$  cardiotoxicity remains to be elucidated. (*Am J Pathol* 2007, 171:463–472; DOI: 10.2353/ajpath.2007.060906)**

Chronic heart failure (CHF) is a consequence of cardiac remodeling processes that can be induced by various types of heart disease<sup>1</sup> such as infections with cardiotropic microorganisms (certain viruses or parasites), host-versus-graft reactions, toxic agents, or other exogenous noxae. The development of CHF is associated with characteristic activation of the immune system<sup>2–5</sup>; however, the exact mechanisms leading to transition from cardiac disease to heart failure and the precise role of the immune system remain to be elucidated in detail. Typical hallmarks for the involvement of immune mechanisms in CHF pathogenesis are the infiltration of the cardiac tissue by leukocytes and the increased cardiac expression of cytokines. In particular, cardiac as well as serum levels of tumor necrosis factor (TNF)- $\alpha$  are significantly elevated in CHF patients suggesting an influence of this proinflammatory cytokine on disease development.<sup>6–10</sup> The cardiotoxic properties of TNF- $\alpha$  are furthermore supported by a characteristic phenotype of TNF- $\alpha$ -overexpressing transgenic mice.<sup>11,12</sup>

Interferon (IFN)- $\gamma$  is another important proinflammatory cytokine with pleiotropic biological effects. Produced by Th1 cells, its most prominent functions are the up-regulation of MHC class I and class II molecules, eventually

Supported by the Stiftung Rheinland-Pfalz für Innovation (grant 8312-38 62 61/527).

K.R. and H.-A.L. contributed equally to this study.

Accepted for publication May 8, 2007.

Address reprint requests to Dr. Kurt Reifenberg, Central Laboratory Animal Facility, Johannes Gutenberg-University, Obere Zahlbacher Str. 67 (Hochhaus am Augustusplatz), D-55131 Mainz, Germany. E-mail: reifenbe@uni-mainz.de.

leading to 1) high-level antigen presentation, 2) suppression of Th2 immune responses, and 3) activation of macrophages.<sup>13–15</sup> To date, the role of IFN- $\gamma$  in the development of human CHF has not been investigated. In Chagas' disease, T cells prepared from patients exhibit an increased parasite-specific IFN- $\gamma$  response, and intensive IFN- $\gamma$  signaling has been demonstrated in the hearts of these patients.<sup>10,16</sup> It has hence been proposed that IFN- $\gamma$  contributes to disease progression from acute cardiac *Trypanosoma* infection to chronic Chagas' cardiomyopathy.<sup>10,16,17</sup> There is clinical evidence that T-cellular IFN- $\gamma$  gene expression is increased in patients with CHF,<sup>18</sup> and Morino and colleagues<sup>19</sup> published a case report of congestive reversible heart failure as a consequence of systemic IFN- $\gamma$  therapy in a patient with renal cell carcinoma. The role of IFN- $\gamma$  in viral myocarditis appears to be less clear-cut. On one hand, there is evidence that IFN- $\gamma$  affords protection during the acute stages of virally induced murine myocarditis.<sup>20,21</sup> On the other hand, IFN- $\gamma$  seems to entertain the gradual progression from an acute virus-specific inflammatory reaction to a chronic cardiomyopathy in mice.<sup>22</sup> Similar to the murine model, many cases of human dilated cardiomyopathy probably represent a long-term sequela of myocarditis caused by coxsackievirus and other viruses.<sup>23–28</sup> Hence, there is sufficient reason to consider IFN- $\gamma$  as a candidate cytokine involved in the pathomechanism leading to CHF.

In the present study, we analyzed the cardiac phenotype of SAP-IFN- $\gamma$  transgenic mice, which constitutively express IFN- $\gamma$  in their livers and also show markedly elevated cytokine serum levels.<sup>29</sup> We provide evidence that SAP-IFN- $\gamma$  mice spontaneously develop chronic active myocarditis, characterized by infiltration of T cells, macrophages, and dendritic cells and by expression of MCP1, MIP1- $\alpha$ , interleukin (IL)-12, and TNF- $\alpha$ , eventually culminating in the development of severe cardiomyopathy.

## Materials and Methods

### Mouse Breeds

Production and characteristics of transgenic lineage SAP-IFN- $\gamma$ 5 (here referred to as SAP-IFN- $\gamma$ ) has been described previously.<sup>29</sup> In brief, SAP-IFN- $\gamma$  transgenic mice carry the cDNA of the murine IFN- $\gamma$  gene cloned downstream from the liver-specific promoter of the human serum amyloid P component (SAP) gene. The SAP-IFN- $\gamma$  strain was previously backcrossed to the C57BL/6 (B6) inbred strain<sup>30</sup> and was propagated by mating hemizygous transgenic males with B6 females. Transgenic offspring could be discriminated from their nontransgenic littermates by polymerase chain reaction (PCR) amplification as described previously.<sup>30</sup> Mice were housed in the Central Laboratory Animal Facility of the University of Mainz under specific pathogen-free conditions.

### Histological and Immunohistochemical Analyses

Mice were sacrificed by exposure to CO<sub>2</sub>, and cardiac tissue specimens were fixed in 4% buffered formaldehyde solution or in Bouin's fixative. Sections were immediately embedded in paraffin, and 4- $\mu$ m sections were stained with hematoxylin and eosin (H&E) or the periodic acid-Schiff reaction according to standard protocols. Apoptosis was analyzed using the *in situ* cell death detection kit (Roche, Basel, Switzerland).

Immunohistological staining of the Mac2 and CD3 antigens was performed on Bouin-fixed sections using immunoenzymatic methods. Deparaffinized sections were reacted before antibody incubation with a commercial target unmasking fluid (Dianova, Hamburg, Germany) in a microwave oven. For macrophage staining the sections were incubated overnight with a biotinylated Mac2-specific (CL8942B; Cedarlane-Biozol, Echting, Germany) antibody. For T-cell immunohistochemistry, the slides were incubated with a CD3-specific (CBL1303; Chemicon, Temecula, CA) primary antibody and a biotinylated secondary antibody (CLCC6015, Cedarlane-Biozol). Biotinylated antibodies were counterstained with phosphatase-conjugated streptavidin (DAKO Diagnostika, Hamburg, Germany). Enzyme activity was revealed with naphthol AS-Bi phosphate in combination with hexazotized new fuchsin (Merck, Darmstadt, Germany). As controls, heart tissue from nontransgenic mice were used.

### Immunofluorescence Analyses

Cryosections were prepared from snap-frozen murine hearts and analyzed by immunofluorescence staining. Immunofluorescence was performed using the TSA Cy3 system (Perkin Elmer, Rodgau, Germany) and a fluorescence microscope (Olympus, Melville, NY). In brief, cryosections were fixed in paraformaldehyde for 10 minutes followed by sequential incubation with methanol, avidin/biotin (Vector Laboratories, Burlingame, CA), and protein blocking reagent (DAKO, Wiesbaden, Germany) to eliminate unspecific background staining. Slides were then incubated overnight with primary antibodies specific for CD11c, CD4, B220 (BD Bioscience, Heidelberg, Germany), CD8 (Southern Biotechnology, Birmingham, AL), Mac2 (Cederlane Laboratories, Hornby, ON, Canada). Subsequently, the slides were incubated for 30 minutes at room temperature with biotinylated secondary antibodies (Dianova, Darmstadt, Germany). All samples were finally treated with streptavidin-horseradish peroxidase and stained with tyramide (Cy3) according to the manufacturer's instructions (Perkin Elmer). Before examination, the nuclei were counterstained with Hoechst33342 (Molecular Probes, Eugene, OR).

### RNA Isolation and Quantitative Reverse Transcriptase (RT)-PCR

Total RNA was extracted from heart samples (0.5 to 1.0 g) by acid guanidinium thiocyanate-phenol-chloroform extraction, as described.<sup>31</sup> One-step RT-PCR was

performed in 25- $\mu$ l reactions in a 96-well spectrofluorometric thermal cycler (iCycler; Bio-Rad, München, Germany). For the real-time quantitative RT-PCR analyses (30 minutes at 50°C, 15 minutes at 95°C, and 40 cycles of 15 seconds at 94°C, 60 seconds at 60°C), the following oligonucleotides served as sense and anti-sense primers and TaqMan hybridization probes: Casp3: sense 5'TG-ATGAGGAGATGGCTTGCC3', anti-sense 5'GTGCGGTACAGCTTCAGC3', probe 5'CAAAGGACGGGTCGTG-GTTCATCCAG3'; Casp7: sense 5'ACATTGACGCTAAT-CCCCGC3', anti-sense 5'TTG CCA TGC TCA TTC AGG ATG 3', probe 5'TCCTCTTTGCTTACTCCACGGTCCCA-GGTTATTA3'; IL-12-p40: sense 5'TACTCCGGACGGTTCACGTG3', anti-sense 5'GTCACTGCCCGAGAGTCAG-G3', probe 5'AAGAAACATGGACTTGAAGTTCAACATC-AAGAGCA3'; inducible nitric-oxide synthase: sense 5'-CAGCTGGGCTGTACAAACCTT3', anti-sense 5'CATTG-GAAGTGAAGCGTTTCG3', probe 5'CGGGCAGCCTGT-GAGACCTTTGA3'; Mcp1: sense 5'CTTCTGGCCTGC-TGTTCA3', anti-sense 5'CCAGCCTACTCATTGGGATC-3', probe 5'CTCAGCCAGATGCAGTTAACGCC3'; Mip1- $\alpha$  sense 5'CTGCAACCAAGTCTTCTCAGC3', anti-sense 5'CTGCCTCCAAGACTCTCAGG3', probe 5'ACT-GCCTGCTGCTTCTCCTACAGCC3'; TGF- $\beta$ 1: sense 5'T-GACGTCACTGGAGTTGTACGG3', anti-sense 5'GGTT-CATGTCATGGATGGTGC3', probe 5'TTCAGCGCTCAC-TGCTCTTGTGACAG3'; TNF- $\alpha$  sense 5'CATCTTCTCAA-AATTCGAGTGACAA3', anti-sense 5'TGGGAGTAGACA-AGGTACAACCC3', probe 5'CACGTCGTAGCAAACCA-CCAAGTGA3'; and Pol2A: sense 5'ACCACGTCCAAT-GATATTGTGGAG3', anti-sense 5'ATGTCATAGTGCA-CACAGGAGCG3', probe 5'CTGGGCATTGAGGCTGTG-CGGAA3'.

TaqMan hybridization probes were double-labeled with 6-carboxyfluorescein (FAM) as reporter fluorophore and carboxytetramethyl-rhodamine (TAMRA) as quencher. All primers and dual-labeled probes (5'-FAM, 3'-TAMRA) were purchased from MWG-Biotech (Ebersberg, Germany). Fluorescence was monitored at each 60°C step. Each experimental reaction was performed in triplicate. All primer/probes sets had efficiencies of 100% ( $\pm$ 10%). To calculate the relative expression of caspase 3, caspase 7, IL-12-p40, inducible nitric-oxide synthase, Mcp1, Mip1- $\alpha$ , TGF- $\beta$ 1, and TNF- $\alpha$  mRNA the  $2^{-\Delta\Delta C(T)}$  method<sup>32</sup> was used. C(T) values of mRNA expression were normalized to the C(T) values of Pol2A mRNA. The  $2^{-\Delta\Delta C(T)}$  values of the B6 mice were set to 100% for each mRNA analyzed.

### *Detection of Proinflammatory Cytokines and Biochemical Parameters in Murine Sera*

IL-12p40/p70, IL-6, IL-2, IFN- $\gamma$ , and TNF- $\alpha$  enzyme-linked immunosorbent assay antibodies and recombinant standards were bought from BD Pharmingen (Heidelberg, Germany) and used according to the manufacturer's instructions. The capture antibody was bound onto the Maxisorb (Nunc, Roskilde, Denmark) assay plate overnight at 4°C. The amount of biotinylated detection antibody was determined using streptavidin-conjugated

horseradish peroxidase, an enzyme that interacts with the 3,3',5,5' TMB liquid substrate (Sigma, St. Louis, MO). After stopping of reaction with 2 mol/L H<sub>2</sub>SO<sub>4</sub> the assay was read out at an absorbance of 450 nm with the SpectraFluorPlus reader from Tecan (Crailsheim, Germany). Alanine transaminase, urea, and creatinine concentrations were determined in murine sera with a SCIL Reflovet Plus system (Scil Animal Care Company, Viernheim, Germany).

### *Mouse Echocardiography*

Echocardiographic analyses were performed in anesthesia. Two-dimensional guided M-mode echoes (30 MHz) were obtained from short- and long-axis views at the level of the largest left ventricular (LV) diameter using a VS-VEVO 660/230 high-resolution imaging system (Visualsonics, Toronto, ON, Canada). LV end-diastolic (LVEDD) and end-systolic (LVESD) dimensions were measured from original tracings by using the leading edge convention of the American Society of Echocardiography. Percent fractional shortening (FS), LV mass (LVM), and end-diastolic wall-thickness/cavity ratio (h/r) were calculated as previously described.<sup>33</sup>

### *Statistical Analysis*

Statistical significance was calculated by Student's *t*-test.

## **Results**

### *Transgenic IFN- $\gamma$ Expression Leads to Chronic Active Myocarditis and Cardiomyopathy*

We conducted a long-term histological follow-up study investigating at least six transgenic mice, as well as the same number of nontransgenic controls, at three distinct age levels. Because almost all IFN- $\gamma$ -expressing mice die prematurely at an age of ~6 to 12 months,<sup>29</sup> we decided to analyze the SAP-IFN- $\gamma$  cardiac phenotype at age levels of 2, 4, and 6 months. In hearts obtained from mutant mice of an age of 2 months, we found only minimal alterations characterized by a low-level interstitial mononuclear infiltrate and discrete signs of disseminated cardiomyolysis (not shown). These cardiac alterations were more advanced in the hearts of 4-month-old SAP-IFN- $\gamma$  mice (Figure 1). At an age of 6 months, the SAP-IFN- $\gamma$  hearts exhibited besides enhanced myodegenerative and inflammatory alterations a reactive interstitial fibrosis with deposition of extracellular matrix (Figure 2D, arrows). At this age level, the cardiopathological process culminated in a notable atrophy of the heart musculature, morphologically characterized by drop-out and variation in the size and shape of cardiac muscle fibers (Figure 2, A–D). This phenomenon was more pronounced in hearts taken from moribund animals (Figure 2, E and F), sacrificed at an age of ~10 months. No pathological cardiac changes could be detected in the nontransgenic controls (not shown).

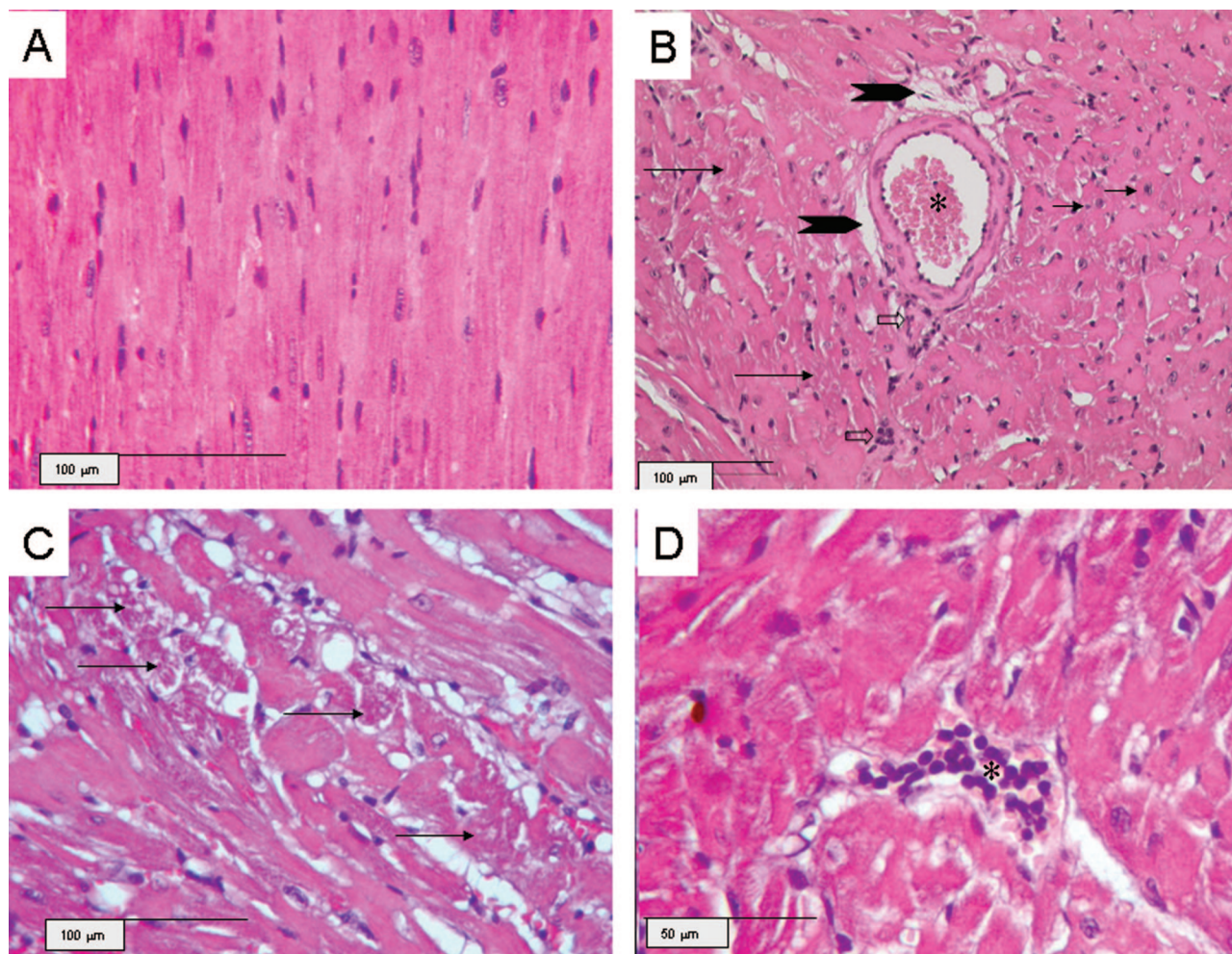


**Figure 1.** Myocardial lesions in 4-month-old SAP-IFN- $\gamma$  transgenic mice. The panels show representative myocardial sections (H&E) of SAP-IFN- $\gamma$  (B–D) and C57BL/6 (B6) mice of an age of 4 months. **A:** C57BL/6 (B6) mouse with normal myocardial histology. **B:** The myocardium of SAP-IFN- $\gamma$  transgenic animals typically exhibits a combination of slight degenerative and mild interstitial inflammatory alterations. Heart muscle fibers vary in their diameters and appear partly shrunken, thereby giving room for a widened (dilated) interstitial space, which becomes especially prominent perivascularly (arrowheads). The asterisk marks the lumen of a penetrating coronary artery with an intact media. Besides degenerating (long black arrows) and regenerating (short black arrows) muscle fibers, paucicellular interstitial infiltrates of mononuclear cells (open arrows) are present. **C:** At higher magnification, degenerating SAP-IFN- $\gamma$  muscle fibers appear heavily vacuolated and contain condensed eosinophilic sarcoplasm (arrows). **D:** A discrete SAP-IFN- $\gamma$  interstitial infiltrate (asterisk) consisting of mononuclear (lymphoid) cells.

Because apoptotic cells had been detected in the cardiac slides of SAP-IFN- $\gamma$  mice of an age of 6 months (Figure 2C), quantitative terminal deoxynucleotidyl transferase dUTP nick-end labeling stainings were performed to investigate this issue further. The mean ( $\pm$ SEM) number of apoptotic cells was found to be increased in the hearts of 6-month-old SAP-IFN- $\gamma$  mice ( $2.3 \pm 0.9$  HPF,  $n = 7$ ) compared with the age-matched controls ( $1.1 \pm 0.4$  HPF,  $n = 7$ ); however, the differences did not attain statistical significance.

#### Cellular Characterization of the SAP-IFN- $\gamma$ Myocarditis

In our next experiment, we analyzed the composition of the cardiac mononuclear infiltrates of the SAP-IFN- $\gamma$

hearts. To this end, cryosections of snap-frozen hearts prepared from 6-month-old SAP-IFN- $\gamma$  mutant and control animals were subjected to immunofluorescence studies. As depicted in Figure 3, the mononuclear infiltrations of SAP-IFN- $\gamma$  mice were comprised of abundant CD4<sup>+</sup> T cells, CD8<sup>+</sup> T cells, Mac2<sup>+</sup> macrophages, and CD11c<sup>+</sup> dendritic cells. In contrast, virtually no B220<sup>+</sup> B could be detected in the hearts of the mutant mice. No notable cellular infiltrate of either cell type was seen in control animals.

Because a previous study<sup>34</sup> has suggested galectin-3 as a relevant marker of activated macrophages in cardiac dysfunction, SAP-IFN- $\gamma$  cardiac slides were immunohistochemically investigated for Mac2<sup>+</sup> (galectin 3<sup>+</sup>) macrophages. Further, CD3-specific immunohistochemical analyses were performed to get a better

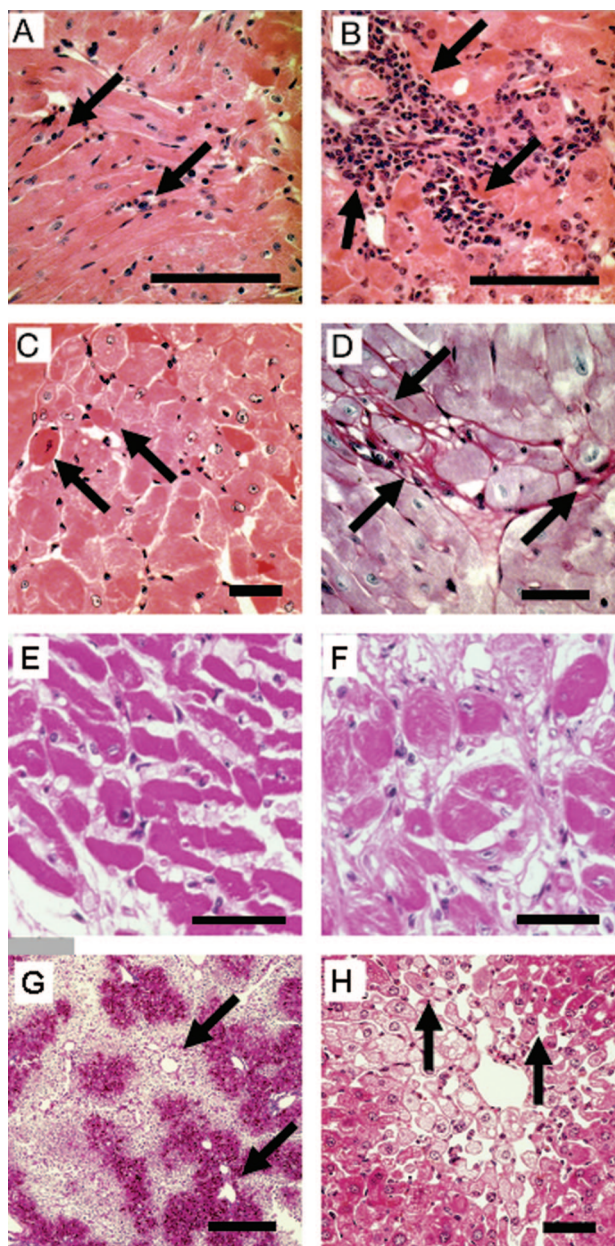


**Figure 2.** Myocarditis and cardiomyopathy in 6-month-old and moribund SAP-IFN- $\gamma$  transgenic mice. **A–F:** Representative longitudinal and cross sections of SAP-IFN- $\gamma$  transgenic hearts of 6-month-old mice (**A–D**) and of moribund (**E**: 10.1-month-old; **F**: 10.5-month-old) animals. At an age of 6 months, systemic IFN- $\gamma$  expression had induced in the SAP-IFN- $\gamma$  hearts (**A, B**; H&E) a variably intensive cardiac inflammatory reaction characterized by abundant infiltration of mononuclear cells (**arrows**). The advanced disease process is further characterized by myofiber apoptosis (**C, arrows**; H&E), cardiomyocellular atrophy and a pronounced fibrosis (**D, arrows**; periodic acid-Schiff). Cardiomyolyses and interstitial fibrosis were accentuated in the subendocardial ventricular myocardium and in the muscular septum of SAP-IFN- $\gamma$  hearts. Note the obvious increase of myofiber atrophy and fibrosis in the hearts of moribund animals (**E, F**; H&E). No cardiac abnormalities could be detected in the age-matched wild-type controls (not shown). **G** and **H:** Venous congestion in the livers of moribund 6-month-old SAP-IFN- $\gamma$  mice (**G, H**; H&E). Note the characteristic liver alterations such as centrolobular dilation of sinusoids (**G, arrows**), trabecular atrophy (**H, arrows**), and centrolobular fatty change (cytoplasmic empty spaces). Scale bars: 200  $\mu$ m (**A, B, E, and G**); 100  $\mu$ m (**C, D, F, and H**).

impression of the cardiac distribution of T cells in SAP-IFN- $\gamma$  hearts. As depicted in Figure 4, the myocardia of SAP-IFN- $\gamma$  mice exhibited significant infiltrations with

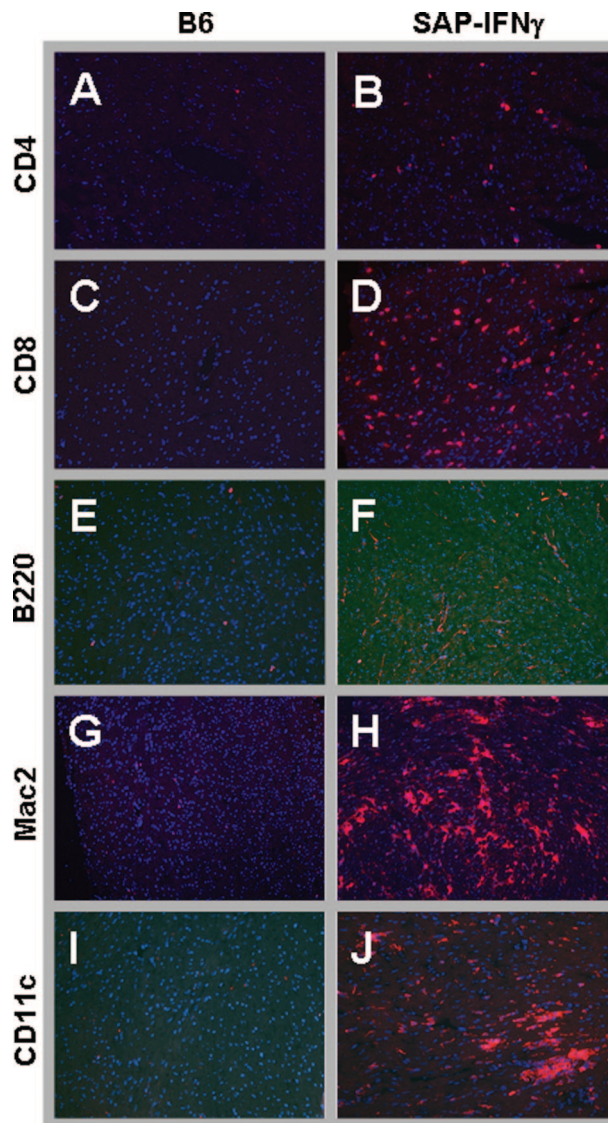


**Figure 3.** Cellular characterization of SAP-IFN- $\gamma$  myocarditis. Snap-frozen hearts prepared from 6-month-old wild-type control mice (left) and of SAP-IFN- $\gamma$  mutants (right) mice were stained with a set of leukocyte-specific antibodies and fluorescent secondary antibodies. Note that the myocarditis of SAP-IFN- $\gamma$  transgenic mice was characterized by significant infiltration of CD4<sup>+</sup> (**B**) and CD8<sup>+</sup> (**D**) T cells, Mac2<sup>+</sup> macrophages (**H**), and CD11c<sup>+</sup> dendritic cells (**J**), whereas virtually no B220<sup>+</sup> B cells (**F**) contributed to the inflammatory reaction. No specific staining reactions could be found in the hearts of the nontransgenic controls (**A, C, E, G, and I**). The immunofluorescence analyses were performed with at least two animals per genotype. Pictures presented show typical staining reactions.

Mac2<sup>+</sup> (galectin 3<sup>+</sup>) macrophages and CD3<sup>+</sup> T cells, whereas the hearts of the B6 controls were free of such infiltrates.

### *IFN- $\gamma$ -Mediated Cardiotoxicity Is Associated with High-Level Expression of Proinflammatory Cytokines*

Because the cytokine TNF- $\alpha$  has a well-documented cardiotoxic potential,<sup>11,12</sup> we speculated that this proinflammatory cytokine might be involved in the pathomechanism underlying SAP-IFN- $\gamma$ -induced cardiomyopathy. To

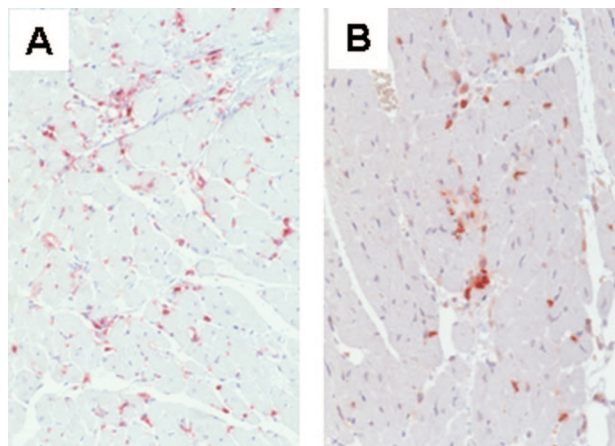


**Figure 4.** Immunohistochemical demonstration of Mac2<sup>+</sup> (=Gal3<sup>+</sup>) macrophages and CD3<sup>+</sup> T cells. Cardiac sections of SAP-IFN- $\gamma$  mice were immunostained for Mac2 (A) and CD3 (B). Note the significant infiltration of the transgenic myocardium by Mac2<sup>+</sup> (=Gal3<sup>+</sup>) macrophages (A) and CD3<sup>+</sup> T cells (B). No such infiltrations could be seen in nontransgenic C57BL/6 controls.

test this hypothesis, we performed quantitative RT-PCR analyses using RNA samples prepared from 6-month-old male SAP-IFN- $\gamma$  mice and age- and sex-matched controls. As depicted in Figure 5, the SAP-IFN- $\gamma$  hearts exhibited a significant increase of transcription of the proinflammatory cytokines TNF- $\alpha$  and IL-12 as well as the macrophage-attracting chemokines MCP1 and MIP1- $\alpha$ . Casp3 and Casp7 transcription was only slightly increased in the SAP-IFN- $\gamma$  hearts, but the differences did not attain statistical significance. No differences of induc-

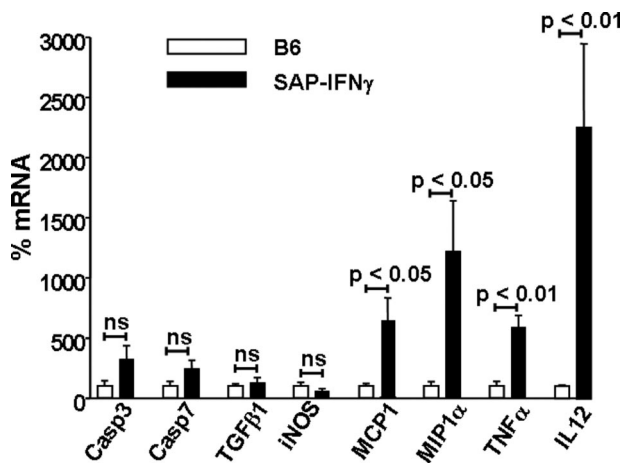


**Figure 5.** Transcription of proinflammatory cytokines and caspases in SAP-IFN- $\gamma$  hearts at an age of 6 months. Total RNA was prepared from the hearts of male SAP-IFN- $\gamma$  ( $n = 8$ ) and C57BL/6 ( $n = 8$ ) mice of an age of 6 months and subjected to quantitative RT-PCR reactions as described in Materials and Methods. Relative expression of caspase 3 (Casp3), caspase 7 (Casp7), TGF- $\beta$ 1, inducible nitric-oxide synthase (iNOS), MCP1, MIP1- $\alpha$ , TNF- $\alpha$ , and IL-12-p40 mRNA was calculated according to the  $2^{-\Delta\Delta C_T}$  method.<sup>32</sup> The  $2^{-\Delta\Delta C_T}$  values of the B6 mice were set to 100%. Note that the SAP-IFN- $\gamma$  hearts exhibited a significant increase of transcription of the macrophage attracting chemokines MCP1 and MIP1- $\alpha$  and the proinflammatory cytokines TNF- $\alpha$  and IL-12 compared with the C57BL/6 (B6) controls. Casp3 and Casp7 transcription was slightly increased in the SAP-IFN- $\gamma$  hearts compared with the nontransgenic counterparts; however, these differences did not attain statistical significance. Data of C57BL/6 mice are shown as black bars, SAP-IFN- $\gamma$  as white bars. The values represent means  $\pm$  SD (ns, not significant).

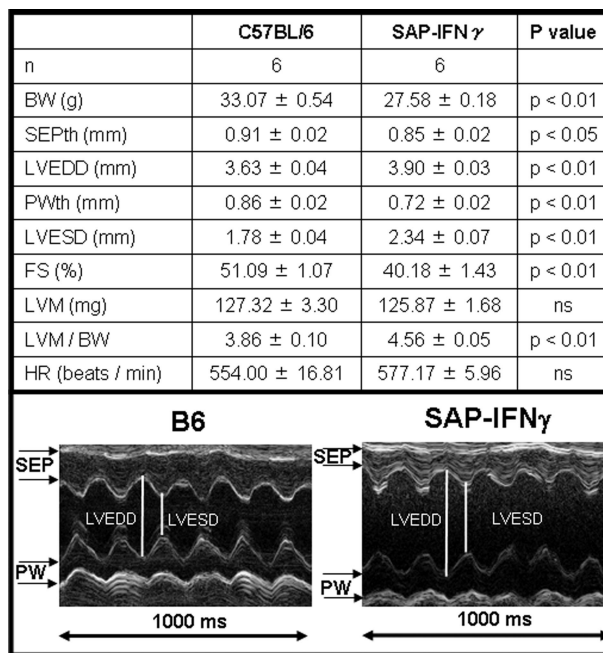


**Figure 6.** Echocardiography. Top: *In vivo* echocardiographic analysis of cardiac size and function in 6-month-old SAP-IFN- $\gamma$  transgenic mice (BW, body weight; SEpth, septal wall thickness; LVEDD, left ventricular end diastolic diameter; PWth, posterior wall thickness; LVESD, left ventricular end systolic diameter; FS, percent fractional shortening calculated as [(LVEDD - LVESD)/LVEDD]  $\times$  100; LVM, left ventricular mass calculated as [1.04  $\times$  (LVEDD + SEpth + PWth)<sup>3</sup> - 0.8  $\times$  LVESD<sup>3</sup> + 0.6]; HR, heart rate, all values: mean  $\pm$  SEM; ns, not significant). Bottom: Representative *in vivo* M-mode echocardiography of a male 6-month-old SAP-IFN- $\gamma$  transgenic mouse (right) and a sex- and age-matched C57BL/6 (B6) control (left). Note that the SAP-IFN- $\gamma$  heart revealed increased LVESD and LVEDD parameters indicating LV dilation and impaired systolic function compared with B6 controls (SEP, interventricular septum; PW, posterior wall).

ible nitric-oxide synthase and TGF- $\beta$ 1 transcription could be detected between SAP-IFN- $\gamma$  and control hearts.

### Impaired Cardiac Function of SAP-IFN- $\gamma$ Mice

Given the significant histological (Figures 1 to 4) and transcriptional (Figure 5) features of myocarditis and cardiomyopathy in SAP-IFN- $\gamma$  mice, it was of great interest to investigate whether IFN- $\gamma$  transgenesis might affect cardiac function. We therefore investigated anesthetized SAP-IFN- $\gamma$  transgenic and B6 control mice of an age of 6 months by echocardiography. As shown in Figure 6 the imaging revealed a significant increase of relative left ventricular mass (LVM/BW) and of left ventricular end diastolic (LVEDD) and end systolic diameter (LVESD) in SAP-IFN- $\gamma$  mice compared with C57BL/6 wild-type controls. Likewise, fractional shortening (FS), interventricular septum (SEpth), and posterior wall (PWth) thickness were decreased in SAP-IFN- $\gamma$  mice compared with B6 controls. Summarizing, the echocardiographic analyses exhibited a LV dilation and impaired systolic function induced by IFN- $\gamma$  overexpression.

To investigate whether the dilated cardiomyopathy, as detectable in SAP-IFN- $\gamma$  mice, might compromise effective blood circulation, we studied the livers of moribund (age of 6 months or higher) SAP-IFN- $\gamma$  mutants for histomorphological signs of congestion. As depicted in Figure

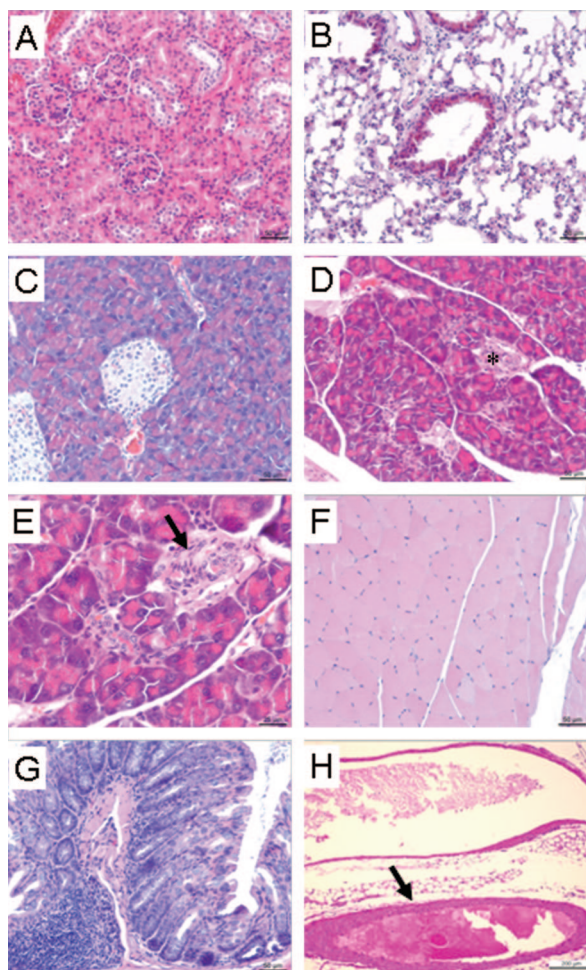


**Figure 7.** Effects of transgenic IFN- $\gamma$  expression on noncardiac organs. Sections (H&E) of various noncardiac organs were prepared from 6-month-old SAP-IFN- $\gamma$  transgenic ( $n = 8$ ) and C57BL/6 ( $n = 8$ ) males and histologically analyzed for pathological lesions. No alterations could be detected in the kidneys (A), lungs (B), femoral musculature (F), duodenum (G), and aorta (H, arrow) of SAP-IFN- $\gamma$  mice. The pancreas of SAP-IFN- $\gamma$  mice exhibited foci of a discrete interstitial, mononuclear infiltrate (D: asterisk; E: higher magnification, arrow), whereas no such infiltrates could be observed in the pancreas of the B6 controls (C).

2, G and H, these mice exhibited congestive liver alterations such as centrilobular, sinusoidal dilatation, trabecular atrophy, and centrilobular fatty degeneration.

### Effects of Constitutive IFN- $\gamma$ Circulation on Noncardiac Organs

In our next experiment, we investigated whether the myocarditis as detectable in SAP-IFN- $\gamma$  hearts could also be detected in other types of musculature. To answer this question we analyzed by microscopic inspection striated skeletal musculature (femoral *Musculus quadriceps*) and various sites of smooth muscle such as large blood vessels (aorta) and the intestinal tract (duodenum) of 6-month-old SAP-IFN- $\gamma$  mutant mice. No inflammatory changes or signs of tissue damage could be observed in any of these tissues (Figure 7, F–H), clearly indicating the myocardiocellular specificity of the pathological process as triggered by the proinflammatory cytokine IFN- $\gamma$ .

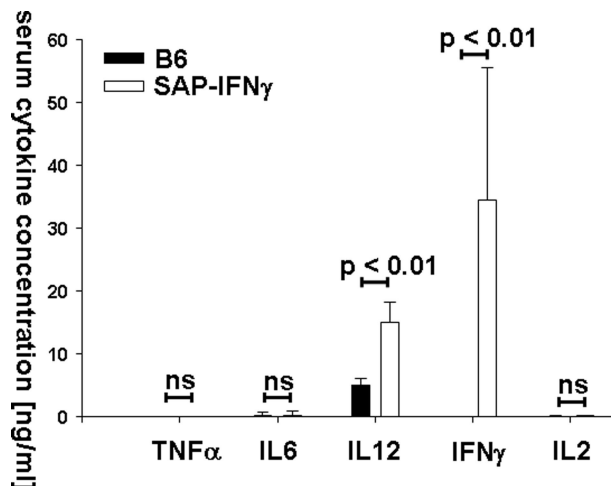


**Figure 8.** Serum concentration of proinflammatory cytokines. Serum was obtained from 6-month-old male SAP-IFN- $\gamma$  ( $n = 9$ ) and C57BL/6 (B6) ( $n = 9$ ) mice and analyzed for proinflammatory cytokine levels by enzyme-linked immunosorbent assay. Note that the concentrations of IFN- $\gamma$  and IL-12p40/p70 were significantly enhanced in SAP-IFN- $\gamma$  mice compared with B6 controls, whereas TNF- $\alpha$ , IL-6, and IL-2 were not. Data of C57BL/6 mice are shown as black bars, SAP-IFN- $\gamma$  as white bars. The values represent means plus SD (ns, not significant).

Further, no pathological abnormalities could be detected in lungs and kidneys of SAP-IFN- $\gamma$  mice (Figure 7, A and B). In full accord with the latter result, the mean ( $\pm$ SEM) serum creatinine (B6, all values  $< 0.5$  mg/dl,  $n = 10$ ; SAP-IFN- $\gamma$ , all values  $< 0.5$  mg/dl,  $n = 10$ ) and urea (B6,  $76.7 \pm 4.5$  mg/dl,  $n = 10$ ; SAP-IFN- $\gamma$ ,  $72.4 \pm 6.3$  mg/dl,  $n = 10$ ) serum concentrations did not differ significantly between both animal groups. In contrast to lungs and kidneys, slight mononuclear infiltrates could be detected in the exocrine pancreas of 6-month-old SAP-IFN- $\gamma$  mice (Figure 7, D and E), whereas no such inflammatory cells could be detected in the age-matched B6 controls (Figure 7C). However, the pancreatic infiltrates as found in SAP-IFN- $\gamma$  transgenic mice only induced minor abnormalities of the exocrine parenchyma, if at all.

Given the inflammatory reactions in pancreata (Figure 7, D and E), hearts (Figures 1 and 2), and livers<sup>29</sup> of SAP-IFN- $\gamma$  mice it was of interest to analyze whether proinflammatory cytokines may be detectable in the serum of such mutants. We therefore investigated the sera of 6-month-old SAP-IFN- $\gamma$  mice and age-matched B6 controls for TNF- $\alpha$ , IL-6, IL-12, IFN- $\gamma$ , and IL-2. As depicted in Figure 8, virtually no TNF- $\alpha$ , IL-6, or IL-2 could be detected in the sera of transgenic or control mice. In full accord with their transgenesis,<sup>29</sup> the SAP-IFN- $\gamma$  mice showed high concentrations of IFN- $\gamma$  in their circulation, whereas this cytokine was not detectable in the serum of B6 mice. Interestingly, the mutant SAP-IFN- $\gamma$  mice exhibited high serum concentrations of IL-12, whereas this cytokine was undetectable in the control sera.

In contrast to a previous report,<sup>29</sup> the SAP-IFN- $\gamma$  variant used in the present study had been adequately backcrossed to the C57BL/6 inbred strain. It was thus of interest to investigate whether the B6 genetic background influenced the hepatic phenotype described previously.<sup>29</sup> However, histological analyses of eight trans-

genic and eight B6 livers prepared at an age of 6 months did not provide any support for this hypothesis (data not shown). Chronic active hepatitis in B6-SAP-IFN- $\gamma$  mice was associated with a significant ( $P < 0.01$ ) elevation of mean ( $\pm$ SEM) alanine transaminase serum concentrations [6-month-old SAP-IFN- $\gamma$  males ( $n = 10$ ), 173.06 U/L  $\pm$  18.2 U/L; age- and sex-matched B6 controls ( $n = 8$ ), 28.32 U/L  $\pm$  1.7 U/L]. The serum alanine transaminase elevation of SAP-IFN- $\gamma$  mice as observed in the current study was adequate to that observed in the previous report.<sup>29</sup>

## Discussion

The principal observation of the present study is that transgenic mice with constitutively elevated IFN- $\gamma$  serum levels develop chronic active myocarditis and cardiomyopathy and thus reveal a hitherto unknown IFN- $\gamma$ -mediated cardiac pathomechanism. We showed that the detrimental IFN- $\gamma$  effect is specifically restricted to the cardiac musculature and that striated and smooth muscles are not affected. To the best of our knowledge, the SAP-IFN- $\gamma$  mice represent the first laboratory experimental model pointing to a cardiotoxic effect of the proinflammatory cytokine IFN- $\gamma$ . We are aware that the expression of IFN- $\gamma$  in the SAP-IFN- $\gamma$  animal model is supraphysiological and leads to a ubiquitous and permanent stimulation of IFN- $\gamma$ -dependent cellular reactions. However, although IFN- $\gamma$  normally shows a paracrine and/or autocrine mode of operation it cannot be excluded that the IFN- $\gamma$  pathomechanisms operative in the murine model are also active in human organs.

The current characterization of the SAP-IFN- $\gamma$  cardiomyopathy mouse model at this point does not allow drawing any final conclusions about the underlying pathomechanism. Because the cardiac disease of SAP-IFN- $\gamma$  transgenic mice is characterized by T-cell infiltrates, it may be speculated that the cardiotoxic IFN- $\gamma$  effect is because of the induction of an autoimmune disease. This hypothesis is supported by experimental observations that autoimmune myocarditis and cardiomyopathy can easily be induced in laboratory mice on immunization with myosin<sup>35,36</sup> and that IFN- $\gamma$  is possibly involved in the development of this autoimmune disease.<sup>37</sup> Involvement of the adaptive immune system into the development of SAP-IFN- $\gamma$  myocarditis is currently being tested by a crossbreeding experiment using the immunodeficient Rag1 strain.<sup>38</sup> However, preliminary data do not point to an essential role of autoimmune mechanisms on the development of SAP-IFN- $\gamma$  cardiac disease.

On the other hand, SAP-IFN- $\gamma$  cardiomyopathy was associated with intensive infiltration by macrophages and dendritic cells and abundant MCP1, MIP1- $\alpha$ , TNF- $\alpha$ , and IL-12 transcription. The abundant presence of macrophage infiltrates in SAP-IFN- $\gamma$  myocardium can be explained by the high expression of the chemokines MCP1 and MIP1- $\alpha$ , which are known to play a major role in the migration of monocytes.<sup>39,40</sup> Our finding of high MCP1 and MIP1- $\alpha$  expression in

SAP-IFN- $\gamma$  hearts is in further accordance with a previous study showing a critical role of these chemokines in the development of murine myocarditis.<sup>41</sup> It can be speculated that IFN- $\gamma$  exerts its cardiotoxic effects in the SAP-IFN- $\gamma$  model by initially activating cardiac macrophages leading to efficient TNF- $\alpha$  and IL-12 synthesis. Activation of cardiac macrophages in SAP-IFN- $\gamma$  mice is impressively underscored by the expression of the galectin-3 marker previously shown to contribute to cardiac dysfunction.<sup>34</sup> TNF- $\alpha$ , which has well-proven cardiotoxic properties,<sup>11,12</sup> could then trigger the cardiomyopathy as observed in SAP-IFN- $\gamma$  mice. Based on this potential pathogenetic mechanism the observed cellular specificity of the IFN- $\gamma$  effect might be explained by the efficient expression of TNF- $\alpha$  receptor molecules by cardiomyocytes.<sup>42,43</sup> However, to the best of our knowledge so far there are no reports about TNF- $\alpha$  receptor density of noncardiac myocytes. If we assume that adaptive immune mechanisms at least in part contribute to SAP-IFN- $\gamma$  cardiomyopathy IL-12 could further aggravate cardiac inflammation by stimulating Th1 responses,<sup>44</sup> as suggested in a previous experimental work.<sup>45</sup> The scenario described above is currently being tested by crossing the SAP-IFN- $\gamma$  transgenic mice to a TNF- $\alpha$  knockout background and by establishing a murine model that allows for the targeted depletion of cardiac macrophages.<sup>46,47</sup>

The RT-PCR analyses conducted in the present study could not discriminate the cellular origin of cardiac TNF- $\alpha$  transcription. Because infiltrating macrophages could be found in SAP-IFN- $\gamma$  cardiomyopathic hearts and because TNF- $\alpha$  synthesis is a typical response of IFN- $\gamma$ -activated macrophages, we expected the cardiac macrophages to predominantly synthesize TNF- $\alpha$  in SAP-IFN- $\gamma$  hearts. However, it should be considered that recent studies have also suggested cardiomyocytes as a potential source of TNF- $\alpha$  biosynthesis.<sup>48,49</sup> The relevance of the dendritic cell infiltrations into the SAP-IFN- $\gamma$  cardiac musculature currently is unclear. The primary effector function of dendritic cells is the regulation of T-cell immunity.<sup>50,51</sup> However, future studies should clarify to what amount SAP-IFN- $\gamma$  cardiomyopathy actually depends on adaptive immunity.

SAP-IFN- $\gamma$  mice die prematurely at an age of 6 to 12 months. In a previous study,<sup>29</sup> it has been speculated that the restricted life span of SAP-IFN- $\gamma$  animals is attributable to infections with gram-negative bacteria. We doubt this hypothesis because the mice used in our experiments were housed under strict specific pathogen-free conditions and because we never observed manifestations of such disease in moribund animals. In our opinion, the most plausible explanation for the premature death of SAP-IFN- $\gamma$  mice is heart failure.

It remains to be shown whether the pathomechanisms active in SAP-IFN- $\gamma$  cardiomyopathy are also operative in human heart failure. However, further characterization of the SAP-IFN- $\gamma$  cardiac disease may lead to a better understanding of the immune reactions associated with CHF.



## Acknowledgments

We appreciate the excellent technical assistance of Antje Canisius, Carolin Orning, and Françoise Burri.

## References

- Cohn JN, Ferrari R, Sharpe N: Cardiac remodeling—concepts and clinical implications: a consensus paper from an international forum on cardiac remodeling. Behalf of an International Forum on Cardiac Remodeling. *J Am Coll Cardiol* 2000, 35:569–582
- Devaux B, Scholz D, Hirche A, Klovekorn WP, Schaper J: Upregulation of cell adhesion molecules and the presence of low grade inflammation in human chronic heart failure. *Eur Heart J* 1997, 18:470–479
- Paulus WJ: Cytokines and heart failure. *Heart Fail Monit* 2000, 1:50–56
- Mari D, Di Berardino F, Cugno M: Chronic heart failure and the immune system. *Clin Rev Allergy Immunol* 2002, 23:325–340
- Torre-Amione G: Immune activation in chronic heart failure. *Am J Cardiol* 2005, 95:3C–40C
- Levine B, Kalman J, Mayer L, Fillit HM, Packer M: Elevated circulating levels of tumor necrosis factor in severe chronic heart failure. *N Engl J Med* 1990, 323:236–241
- Zhao SP, Zeng LH: Elevated plasma levels of tumor necrosis factor in chronic heart failure with cachexia. *Int J Cardiol* 1997, 58:257–261
- Rauchhaus M, Doehner W, Francis DP, Davos C, Kemp M, Liebenthal C, Niebauer J, Hooper J, Volk HD, Coats AJ, Anker SD: Plasma cytokine parameters and mortality in patients with chronic heart failure. *Circulation* 2000, 102:3060–3067
- Kubota T, Miyagishima M, Alvarez RJ, Kormos R, Rosenblum WD, Demetris AJ, Semigran MJ, Dec GW, Holubkov R, McTiernan CF, Mann DL, Feldman AM, McNamara DM: Expression of proinflammatory cytokines in the failing human heart: comparison of recent-onset and end-stage congestive heart failure. *J Heart Lung Transplant* 2000, 19:819–824
- Cunha-Neto E, Dzau VJ, Allen PD, Stamatou D, Benvenuti L, Higuchi ML, Koyama NS, Silva JS, Kalil J, Liew CC: Cardiac gene expression profiling provides evidence for cytokinopathy as a molecular mechanism in Chagas' disease cardiomyopathy. *Am J Pathol* 2005, 167:305–313
- Kubota T, McTiernan CF, Frye CS, Slawson SE, Lemster BH, Koretsky AP, Demetris AJ, Feldman AM: Dilated cardiomyopathy in transgenic mice with cardiac-specific overexpression of tumor necrosis factor- $\alpha$ . *Circ Res* 1997, 81:627–635
- Bryant D, Becker L, Richardson J, Shelton J, Franco F, Peshock R, Thompson M, Giroir B: Cardiac failure in transgenic mice with myocardial expression of tumor necrosis factor- $\alpha$ . *Circulation* 1998, 97:1375–1381
- Strehl B, Seifert U, Kruger E, Heink S, Kuckelkorn U, Kloetzel PM: Interferon- $\gamma$ , the functional plasticity of the ubiquitin-proteasome system, and MHC class I antigen processing. *Immunol Rev* 2005, 207:19–30
- Mosmann TR, Coffman RL: TH1 and TH2 cells: different patterns of lymphokine secretion lead to different functional properties. *Annu Rev Immunol* 1989, 7:145–173
- Ma J, Chen T, Mandelin J, Ceponis A, Miller NE, Hukkanen M, Ma GF, Kontinen YT: Regulation of macrophage activation. *Cell Mol Life Sci* 2003, 60:2334–2346
- Abel LC, Rizzo LV, Ianni B, Albuquerque F, Bacal F, Carrara D, Bocchi EA, Teixeira HC, Mady C, Kalil J, Cunha-Neto E: Chronic Chagas' disease cardiomyopathy patients display an increased IFN- $\gamma$  response to *Trypanosoma cruzi* infection. *J Autoimmun* 2001, 17:99–107
- Gomes JA, Bahia-Oliveira LM, Rocha MO, Martins-Filho OA, Gazzinelli G, Correa-Oliveira R: Evidence that development of severe cardiomyopathy in human Chagas' disease is due to a Th1-specific immune response. *Infect Immun* 2003, 71:1185–1193
- Yndestad A, Holm AM, Muller F, Simonsen S, Froland SS, Gullestad L, Aukrust P: Enhanced expression of inflammatory cytokines and activation markers in T-cells from patients with chronic heart failure. *Cardiovasc Res* 2003, 60:141–146
- Morino Y, Hara K, Ushikoshi H, Tanabe K, Kuroda Y, Noguchi T, Ayabe S, Hara H, Yanbe Y, Kozuma K, Ikari Y, Saeki F, Tamura T:  $\gamma$ -Interferon-induced cardiomyopathy during treatment of renal cell carcinoma: a case report. *J Cardiol* 2000, 36:49–57
- Horwitz MS, La Cava A, Fine C, Rodriguez E, Ilic A, Sarvetnick N: Pancreatic expression of interferon-gamma protects mice from lethal coxsackievirus B3 infection and subsequent myocarditis. *Nat Med* 2000, 6:693–697
- Fairweather D, Frisnacho-Kiss S, Yusung SA, Barrett MA, Davis SE, Gatewood SJ, Njoku DB, Rose NR: Interferon- $\gamma$  protects against chronic viral myocarditis by reducing mast cell degranulation, fibrosis, and the profibrotic cytokines transforming growth factor- $\beta$ 1, interleukin-1 $\beta$ , and interleukin-4 in the heart. *Am J Pathol* 2004, 165:1883–1894
- Shioi T, Matsumori A, Sasayama S: Persistent expression of cytokine in the chronic stage of viral myocarditis in mice. *Circulation* 1996, 94:2930–2937
- MacArthur CG, Tarin D, Goodwin JF, Hallidie-Smith KA: The relationship of myocarditis to dilated cardiomyopathy. *Eur Heart J* 1984, 5:1023–1035
- Baboonian C, Davies MJ, Booth JC, McKenna WJ: Coxsackie B viruses and human heart disease. *Curr Top Microbiol Immunol* 1997, 223:31–52
- Hill SL, Rose NR: The transition from viral to autoimmune myocarditis. *Autoimmunity* 2001, 34:169–176
- Feldman AM, McNamara D: Myocarditis. *N Engl J Med* 2000, 343:1388–1398
- Noutsias M, Pauschinger M, Poller WC, Schultheiss HP, Kuhl U: Immunomodulatory treatment strategies in inflammatory cardiomyopathy: current status and future perspectives. *Expert Rev Cardiovasc Ther* 2004, 2:37–51
- Rutschow S, Li J, Schultheiss HP, Pauschinger M: Myocardial proteases and matrix remodeling in inflammatory heart disease. *Cardiovasc Res* 2006, 69:646–656
- Toyonaga T, Hino O, Sugai S, Wakasugi S, Abe K, Shichiri M, Yamamura K: Chronic active hepatitis in transgenic mice expressing interferon- $\gamma$  in the liver. *Proc Natl Acad Sci USA* 1994, 91:614–618
- Merkle H, Nusser P, Knehr S, Lohler J, Barsig J, Yamamura KI, Reifenberg K: Hepatocytes of double-transgenic mice expressing high levels of hepatitis B virus e antigen and interferon- $\gamma$  are not injured by HBeAg specific autoantibodies. *Arch Virol* 2000, 145:1081–1098
- Chomczynski P, Sacchi N: Single-step method of RNA isolation by acid guanidinium thiocyanate-phenol-chloroform extraction. *Anal Biochem* 1987, 162:156–159
- Livak KJ, Schmittgen TD: Analysis of relative gene expression data using real-time quantitative PCR and the  $2^{-\Delta\Delta C_T}$  method. *Methods* 2001, 25:402–408
- Schmidt AG, Kadambi VJ, Ball N, Sato Y, Walsh RA, Kranias EG, Hoit BD: Cardiac-specific overexpression of caldesmon results in left ventricular hypertrophy, depressed force-frequency relation and pulsus alternans in vivo. *J Mol Cell Cardiol* 2000, 32:1735–1744
- Sharma UC, Pokharel S, van Brakel TJ, van Berlo JH, Cleutjens JP, Schroen B, Andre S, Crijns HJ, Gahuis HJ, Maessen J, Pinto YM: Galectin-3 marks activated macrophages in failure-prone hypertrophied hearts and contributes to cardiac dysfunction. *Circulation* 2004, 110:3121–3128
- Afanasyeva M, Wang Y, Kaya Z, Park S, Zilliox MJ, Schofield BH, Hill SL, Rose NR: Experimental autoimmune myocarditis in A/J mice is an interleukin-4-dependent disease with a Th2 phenotype. *Am J Pathol* 2001, 159:193–203
- Eriksson U, Kurrer MO, Bingisser R, Eugster HP, Saremaslani P, Follath F, Marsch S, Widmer U: Lethal autoimmune myocarditis in interferon- $\gamma$  receptor-deficient mice: enhanced disease severity by impaired inducible nitric oxide synthase induction. *Circulation* 2001, 103:18–21
- Smith SC, Allen PM: Neutralization of endogenous tumor necrosis factor ameliorates the severity of myosin-induced myocarditis. *Circ Res* 1992, 70:856–863
- Mombaerts P, Iacomini J, Johnson RS, Herrup K, Tonegawa S, Pa-paioannou VE: RAG-1-deficient mice have no mature B and T lymphocytes. *Cell* 1992, 68:869–877
- Lu B, Rutledge BJ, Gu L, Fiorillo J, Lukacs NW, Kunkel SL, North R, Gerard C, Rollins BJ: Abnormalities in monocyte recruitment and

- cytokine expression in monocyte chemoattractant protein 1-deficient mice. *J Exp Med* 1998, 187:601–608
40. Maekawa N, Wada H, Kanda T, Niwa T, Yamada Y, Saito K, Fujiwara H, Sekikawa K, Seishima M: Improved myocardial ischemia/reperfusion injury in mice lacking tumor necrosis factor- $\alpha$ . *J Am Coll Cardiol* 2002, 39:1229–1235
  41. Göser S, Ottl R, Brodner A, Dengler TJ, Torzewski J, Egashira K, Rose NR, Katus HA, Kaya Z: Critical role for monocyte chemoattractant protein-1 and macrophage inflammatory protein-1 $\alpha$  in induction of experimental autoimmune myocarditis and effective anti-monocyte chemoattractant protein-1 gene therapy. *Circulation* 2005, 112:3400–3407
  42. Higuchi Y, McTiernan CF, Frye CB, McGowan BS, Chan TO, Feldman AM: Tumor necrosis factor receptors 1 and 2 differentially regulate survival, cardiac dysfunction, and remodeling in transgenic mice with tumor necrosis factor-alpha-induced cardiomyopathy. *Circulation* 2004, 109:1892–1897
  43. Torre-Amione G, Kapadia S, Lee J, Bies RD, Lebovitz R, Mann DL: Expression and functional significance of tumor necrosis factor receptors in human myocardium. *Circulation* 1995, 92:1487–1493
  44. Szabo SJ, Sullivan BM, Peng SL, Glimcher LH: Molecular mechanisms regulating Th1 immune responses. *Annu Rev Immunol* 2003, 21:713–758
  45. Afanasyeva M, Wang Y, Kaya Z, Stafford EA, Dohmen KM, Sadighi Akha AA, Rose NR: Interleukin-12 receptor/STAT4 signaling is required for the development of autoimmune myocarditis in mice by an interferon- $\gamma$ -independent pathway. *Circulation* 2001, 104:3145–3151
  46. Buch T, Heppner FL, Tertilt C, Heinen TJ, Kremer M, Wunderlich FT, Jung S, Waisman A: A Cre-inducible diphtheria toxin receptor mediates cell lineage ablation after toxin administration. *Nat Methods* 2005, 2:419–426
  47. Clausen BE, Burkhardt C, Reith W, Renkawitz R, Forster I: Conditional gene targeting in macrophages and granulocytes using LysMcre mice. *Transgenic Res* 1999, 8:265–277
  48. Giroir BP, Johnson JH, Brown T, Allen GL, Beutler B: The tissue distribution of tumor necrosis factor biosynthesis during endotoxemia. *J Clin Invest* 1992, 90:693–698
  49. Kapadia S, Lee J, Torre-Amione G, Birdsall HH, Ma TS, Mann DL: Tumor necrosis factor-alpha gene and protein expression in adult feline myocardium after endotoxin administration. *J Clin Invest* 1995, 96:1042–1052
  50. Adams S, O'Neill DW, Bhardwaj N: Recent advances in dendritic cell biology. *J Clin Immunol* 2005, 25:177–188
  51. Banchereau J, Palucka AK: Dendritic cells as therapeutic vaccines against cancer. *Nat Rev Immunol* 2005, 5:296–306